Since January 2020 Elsevier has created a COVID-19 resource centre with free information in English and Mandarin on the novel coronavirus COVID-19. The COVID-19 resource centre is hosted on Elsevier Connect, the company's public news and information website.

Journal of Loss Prevention in the Process Industries 69 (2021) 104336

Contents lists available at ScienceDirect

Journal of Loss Prevention in the Process Industries

journal homepage: http://www.elsevier.com/locate/jlp

Modeling aerosol transmission of SARS-CoV-2 in multi-room facility

Matthew Kennedy *, Sung Jin Lee, Michael Epstein

Fauske & Associates, LLC, Burr Ridge, IL, USA

ARTICLE INFO

Keywords:
Airborne transmission
SARS-CoV-2 transmission
SARS-CoV-2 infection
COVID 19
Facility modeling

ABSTRACT

The versatile and computationally attractive FATE™ facility software package for analyzing the transient behavior of facilities during normal and off-normal conditions is applied to the problem of SARS-CoV-2 virus transmission in single-and multi-room facilities. Subject to the justifiable assumptions of non-interacting virus droplets, room-wide spatially homogeneous virus droplet aerosols and droplet sedimentation in accordance with Stokes law; the FATE code tracks the virus aerosol from a human source through a facility with a practical ventilation system which reconditions, filters, and recycles the air. The results show that infection risk can be reduced by 50 percent for increased facility airflow, 70 percent for increased airflow and the inclusion of a HEPA filter on recirculated ventilation air, and nearly 90 percent for increased airflow, inclusion of a HEPA filter, and wearing a mask. These results clearly indicate that there are operational changes and engineering measures which can reduce the potential infection risk in multi-room facilities.

1. Introduction

The global health pandemic of 2020 caused by SARS-CoV-2, the virus that causes COVID-19, has challenged many individuals and organizations to re-think everyday tasks. As the world begins to return to normal, business, companies, and organizations are re-evaulating their preparedness for minimizing the spread of infection as customers and employees return. One critical feature that is vital for a safe return to normal is an understanding of how SARS-CoV-2 is transmitted within a facility. The World Health Organization (2020) released a scientific brief, noting that research on the topic is still ongoing, that transmission occurs by:

1. Contact and droplet transmission
2. Airborne (aerosol) transmission
3. Fomite (contaminated surfaces) transmission

This paper contributes to the body of knowledge regarding airborne transmission of SARS-CoV-2 by aerosol virus particles within a building containing interconnected, well-mixed regions. The analysis performed in this paper, using Fauske & Associates, LLC FATE software program, suggests that there are actions that businesses, companies, and organizations can take to reduce the potential transmission between individuals by reducing the amount of virus aerosols within the building. It is noted that this paper does not touch upon the topics of social distancing and frequent hand washing which are important aspects of reducing the spread of the virus. While these topics are important for droplet and surface transmission, they are considered outside the scope of this paper focused on aerosol transmission. Aerosol transmission by inhaling indoor air loaded with uniformly distributed virus aerosols is considered. The paper focuses on a constant aerosol generation, through normal breathing, resulting in a quasi-steady state viral load within the facility. Aerosol transmission in the near field close to the viral shedding human source or sporadic aerosol generation through coughing or sneezing is not evaluated as part of this effort.

2. Model overview

2.1. FATE overview

The FATE (Flow Aerosol Thermal and Explosion) Facility software package is a versatile program for analyzing the transient behavior of facilities and systems during normal and off-normal conditions. It has traditionally been used for modeling fire and smoke transport, hydrogen production and migration, as well as predicting pressure and temperature behavior of nuclear waste during packaging, drying, transport, and storage.

A unique feature of FATE is its ability to characterize and track aerosols including deposition from settling, impaction, and filtration. This feature has typically been used to quantify the potential hazard to

* Corresponding author.
E-mail address: kennedy@fauske.com (M. Kennedy).

https://doi.org/10.1016/j.jlp.2020.104336
Received 26 August 2020; Received in revised form 19 October 2020; Accepted 26 October 2020
Available online 5 November 2020

personnel and the public from the hazardous aerosol particulate released under off-normal conditions. This is done by tracking the transport of aerosol particles from a source (accident location) through the facility and into the environment while accounting for any settling, impaction, or filtration which may occur. While the FATE software package has been historically used to model industrial hazards (chemical and radiological) it is generic enough that it can model biological aerosols, such as SARS-CoV-2. The following two sub-sections provide a description of the applicability of FATE's aerosol modeling for biological scenarios.

2.2. Criteria for spatially homogeneous aerosol assumption

Two room-air-mixing mechanisms that can potentially support a spatially homogeneous virus droplet aerosol are (i) natural-convection-driven mixing due to the walls of the room being warmer or colder than the bulk room air and (ii) mixing due to a ventilation system that supplies outside air to the room through an inlet vent and removes room air through an exhaust vent.

One can use a Lagrangian approach to follow the motion of a droplet of a given size in the room environment. If the droplet trajectory is such that it travels around the room before falling out as it passes over the floor, then droplets of this size tend to form a spatially homogenous aerosol. The calculation of droplet trajectories requires knowledge of the room-air-flow pattern. An alternative and roughly equivalent approach to a criterion for a spatially homogeneous aerosol is to calculate the time t_{circ} it takes for the mixing mechanism to circulate (pump) one room-air volume. Then the criterion for a spatially uniform virus droplet aerosol takes the form

$$t_{circ} \ll t_{sed} \tag{1}$$

where t_{sed} is the time it takes for a virus droplet to traverse the height H of the room by gravitational settling:

$$t_{sed} = \frac{H}{v_{sed}} \tag{2}$$

In Eq. (2), v_{sed} is the droplet sedimentation velocity.

There is an inconsistency to the criterion given by Eq. (1) in that the left-hand-side pertains to very small droplets that follow the airflow streamlines, whereas the right-hand-side pertains to droplets that are large enough to be uninfluenced by the room air flow and follow a nearly vertical path to the floor of the room. This is the rough nature of the criterion, but the requirement that the droplet circulation time be much smaller than the settling time should help to neutralize the inconsistency.

2.2.1. Natural convection

Cheesewright (1968) measured the velocity profiles across the width of a turbulent natural convection boundary layer on a vertical surface. From his measurements one can show that the volumetric flow of air Q_{nc} (in $m^3\ s^{-1}$) "pumped" by the turbulent boundary layer is

$$Q_{nc} = 0.0931\ \ W\ \ \nu Gr^{0.4}, \tag{3}$$

where Gr is the Grashof number:

$$Gr = \frac{g\Delta T H^3}{T\nu^2} \tag{4}$$

In Eqs. (3) and (4), W is the width of the boundary layer (or perimeter of the room), H is the height of the boundary layer (or room height), ν and T are the kinematic viscosity and temperature of the room air, respectively, g is the gravitational constant, and ΔT is the temperature difference between the walls and the room air.

It follows that for natural convection air pumping, the air circulation time in a room of volume V is

$$t_{circ} = \frac{V}{Q_{nc}}, \tag{5}$$

and, therefore, the criterion for a spatially homogeneous aerosol is (see Eqs. (1) and (2))

$$\frac{V v_{sed}}{H Q_{nc}} \ll 1 \tag{6}$$

The sedimentation velocity v_{sed} in Eq. (6) of a droplet of diameter d may be accurately estimated using the following equation (Epstein, 2002):

$$v_{sed} = \frac{\nu \mathrm{Re}}{d} \tag{7}$$

where Re is a Reynolds number function of a dimensionless parameter ω, which is the ratio of the Stoke's law droplet settling velocity to the velocity ν/d that appears in Eq. (7). Specifically,

$$\omega = \frac{d^3 \rho_l \rho g}{18\mu^2}, \tag{8}$$

and Re is related to ω by

$$\mathrm{Re} = \frac{\omega}{\left[1 + 0.2268\omega^{0.5216}\right]^{0.7669}} \tag{9}$$

In Eq. (8), μ and ρ are the viscosity and density of the room air, respectively, and ρ_l is the density of the droplet.

Table 1 lists values of V v_{sed}/(HQ_{nc}) as a function of the virus-containing droplet diameter d for ΔT = 1.0, 5.0 K; for a room of dimensions V = 680 m^3, H = 3.66 m, W = 54.5 m, and air temperature T = 293 K. The remaining pertinent parameter values are $\rho_l = 10^3\ kg\ m^{-3}$, $\rho = 1.21\ kg\ m^{-3}$, $\mu = 1.82 \times 10^{-5}\ kg\ m^{-1}\ s^{-1}$ and $\nu = 1.51 \times 10^{-5}\ m^2\ s^{-1}$. The predicted natural-convection-driven volumetric air flow rates (see Eqs. (3) and (4)) used in the construction of Table 1 are

$$Q_{nc} = 0.672 m^3 s^{-1}, \quad \text{for} \quad \Delta T = 1.0K \tag{10}$$

$$Q_{nc} = 1.278 m^3 s^{-1}, \quad \text{for} \quad \Delta T = 5.0K \tag{11}$$

It is clear from Table 1 that, according to the criterion presented here (Eq. (6)), it is difficult to justify the spatially homogeneous aerosol assumption for droplet sizes greater than approximately 10 μm. Coughing and sneezing yields droplets that are 50 μm or larger (Asadi et al., 2019). However, the size of the droplets generated during breathing and normal speech are much smaller, about 1.0 μm, and these droplets most certainly satisfy Eq. (6) for a spatially homogeneous aerosol in a naturally-convected room atmosphere. Given the intent to prevent transmission of the virus prior to human vectors presenting detectable symptoms such as coughing or sneezing, or when they remain asymptomatic but contagious, this paper provides a meaningful analysis of the spatially homogeneous aerosol.

2.2.2. Forced air ventilation

Suppose air enters the room with a velocity u_o through a circular air inlet vent of radius R_o. Assuming the vent is located in the ceiling, from the theory of momentum jets the room air flow rate Q_{vent} pumped by the intake flow rate Q_o is

Table 1
Spatially Homogeneous Aerosol Factor V v_{sed}/(HQ_{nc}) as a Function of Aerosol Droplet Diameter d.

d (μm)	v_{sed} ($m\ s^{-1}$)	$\frac{Vv_{sed}}{HQ_{nc}}$(ΔT = 1.0 K)	$\frac{Vv_{sed}}{HQ_{nc}}$(ΔT = 5.0 K)
1.0	2.99×10^{-5}	8.27×10^{-3}	4.35×10^{-3}
5.0	7.48×10^{-4}	0.206	0.109
10.0	2.98×10^{-3}	0.823	0.433
20.0	1.17×10^{-2}	3.23	1.70

$$Q_{vent} = Q_o + 2\pi E_o R_o H u_o \tag{12}$$

where the last term is the flow rate of room air entrained by the intake ventilation jet. The parameter E_o in Eq. (12) is an empirical entrainment coefficient of value approximately 0.08. The room air circulation time is

$$t_{circ} = \frac{V}{Q_{vent}} \tag{13}$$

It follows then, from Eqs. (1) and (2), that the condition for the existence of a spatially homogeneous aerosol is

$$\frac{V v_{sed}}{H Q_{vent}} \ll 1 \tag{14}$$

Consider the 680 m^3 room of the previous example connected to a ventilation system that supplies four room volume air changes per hour; that is, $Q_o = 0.756\ m^3\ s^{-1}$. The radius of the inlet vent is taken to be $R_o = 0.4$ m (0.503 m^2) and, therefore, the air enters the room with velocity $u_o = 1.5\ m\ s^{-1}$. From Eq. (12), the ventilation flow circulates the room air at the rate

$$Q_{vent} = 1.86 m^3 s^{-1} \tag{15}$$

This circulation flow rate is of the same order as Q_{nc} predicted for a sealed room with circulation flow due to natural convection (see Eqs. (10) and (11)). Thus, for the room air ventilation system parameters selected, ventilation flow is capable of supporting a spatially homogeneous aerosol generated by normal speech, but not an aerosol produced by coughing and sneezing.

It is noted that the combination of an outlet vent and the fact that a human generated aerosol is extremely sparse (see next section) may prevent a spatially homogeneous aerosol from forming regardless of whether or not Eq. (14) is satisfied. Depending on the position of the human source, the aerosol droplets may be transported directly to the outlet vent before they can circulate around the room. A Lagrangian droplet trajectory analysis may be the only way of determining if a spatially homogeneous aerosol is possible for a given human source location within a ventilated room.

2.3. Aerosol sedimentation in the FATE software

In FATE the deposition rate of aerosol is calculated one of two ways depending on the aerosol mass concentration. When the aerosol concentration is sufficient or there are large aerosol generation sources, coagulation is significant, and sedimentation is accounted for based on the correlation method developed by Epstein et al. (1986 and 1988). Correlations implicitly account for particle size distribution. The correlation method is accurate as long as substantial coagulation occurs before significant droplet sedimentation takes place. Dilute aerosols of slowly agglomerating droplets fail to satisfy this requirement. In mathematical terms, the correlation method breaks down when the droplet source rate $\dot{m}_d$ (kg s^{-1}) obeys the inequality (Epstein et al., 1986).

$$\dot{m}_d \lesssim 10^{-2} V \left(\frac{g K_o^3 \rho_l^5}{\mu H^8} \right)^{1/4} \tag{16}$$

where K_o is a Brownian collision coefficient equal to approximately $2.96 \times 10^{-16}\ m^3\ s^{-1}$ for room temperature air. For the example room problem treated earlier, the right-hand-side of Eq. (16) is 1.75×10^{-7} kg s^{-1}. A typical human aerosol source rate is orders of magnitude below this value, say, $\dot{m}_d \sim 10^{-13} kgs^{-1}$. Clearly, droplets emitted during breathing, coughing, etc., when spread out over the volume of a typical room, result in non-interacting droplets.

Another way of considering the possibility of virus droplet collisions is to estimate the mean free path λ between droplets. A simple solution for λ can be obtained for a monodisperse virus droplet aerosol under steady-state conditions. In this special case all the aerosol droplets deposit at the same velocity v_{sed}. Equating the mass rate of aerosol generation $\dot{m}_d$ to the mass rate of deposition yields

$$\dot{m}_d = \frac{\pi}{6} d^3 \rho_l N v_{sed} A \tag{17}$$

where N is the aerosol droplet number density (droplets per spatial volume) and A is the floor area for droplet deposition (A = V/H). The mean free path λ between droplets is related to N as follows:

$$\frac{4}{3}\pi\lambda^3 = \frac{1}{N} \tag{18}$$

Eliminating N between Eqs. (17) and (18) and solving the result for λ yields

$$\lambda = \frac{d}{2} \left(\frac{\rho_l v_{sed} V}{\dot{m}_d H} \right)^{1/3} \tag{19}$$

Once again returning to our example room, V = 680 m^3 and H = 3.66 m. A 10 μm droplet deposits on the floor of the room with velocity $v_{sed} = 2.98 \times 10^{-3}$ m-s^{-1} (see Table 1). Inserting these parameter values, together with the typical human aerosol mass generation rate $\dot{m}_d = 10^{-13} kgs^{-1}$, into Eq. (19) gives

$$\lambda = 0.88m \tag{20}$$

Indeed, the separation distance between droplets is so large that droplet collisions cannot occur. For 1.0 μm droplets $v_{sed} = 2.99 \times 10^{-5}$ m s^{-1} and $\lambda = 1.91 \times 10^{-2}$ m. At first glance this mean free path seems small enough for droplet collisions to occur. But this is not the case since the mean free path is more than four decades larger than the droplet diameter ($\lambda/d = 1.91 \times 10^4$). The probability of one droplet colliding with another droplet is virtually zero.

When the aerosol concentration is not significant and droplets are non-interacting, the aerosol is said to be sparse and the deposition rate can be determined from Stoke's law for particle settling velocity. In FATE the user can invoke the sparse aerosol model. Using the sparse aerosol model the deposition rate is determined assuming a log-normal aerosol size distribution. The user inputs the geometric mean and geometric standard deviation factor of the aerosol source. The code tracks its transport, settling, and evolving log-normal size distribution.

3. SARS-CoV-2 inputs and assumptions

The airborne viral emission rate of SARS-CoV-2 estimated by Buonanno et al. (2020), and described here, is used. The droplet size and concentration in exhaled air for different activities (i.e. breathing, whispered counting, voiced counting, and unmodulated vocalization) were measured by Morawska et al. (2009). In this study a particle size distribution with four channels was considered as shown in Table 2. The total volume of droplets in a cubic centimeter of exhaled air is estimated by the product of droplet number density and volume of a sphere with the diameter of the droplet. The last column in Table 2 shows the droplet volume density.

Table 2
Droplet Concentration (cm^{-3}) of the Aerosol Modes during each Expiratory Activity (Morawska et al., 2009) (the last column is added by this paper).

Expiratory activity	D_1 (0.80 μm)	D_2 (1.8 μm)	D_3 (3.5 μm)	D_3 (5.5 μm)	Aerosol concentration in exhaled air, mL cm^{-3}
Voiced counting	0.236	0.068	0.007	0.011	1.39×10^{-12}
Whispered counting	0.110	0.014	0.004	0.002	3.36×10^{-13}
Unmodulated vocalization	0.751	0.139	0.139	0.059	8.89×10^{-12}
Breathing	0.084	0.009	0.003	0.002	2.92×10^{-13}

Adams (1993) reported inhalation rates for five different activity levels as shown in Table 3.

For the virus aerosol source, a SARS-CoV-2 emitter with the inhalation rate of light exercise and the expiratory activity of speaking (considered as the mean value between unmodulated vocalization and voiced counting, 5.14×10^{-12} mL cm^{-3}) is considered. The corresponding virus aerosol source rate is 7.09×10^{-6} mL h^{-1}. Assuming the density of water, 1000 kg m^{-3}, the mass source rate of the virus aerosol is 2.0×10^{-12} kg s^{-1}, an input to the FATE model. The geometric mean and standard deviation of 1.51 μm and 2.01 are assumed for the droplet size distribution in this paper.

The half-life of SARS-CoV-2 in aerosols is estimated to be 1.1–1.2 h with 95% credible interval of 0.64–2.64 h (van Doremalen et al., 2020). A half-life of 1.1 h is assumed in this paper. Deactivation of airborne virus is represented in the FATE model using a pair of purge flows in each region that removes aerosols at the rate equivalent to the virus deactivation rate. For a room with a free volume of 135.9 cubic meter, the volumetric purge flow rate that will remove aerosols with a half-life of 1.1 h is given by ln(2)/(1.1 × 3600) x 135.9 m^3/s, or 0.0238 m^3/s. The purge flow junctions are not shown in Figs. 1 and 4.

For the individuals of interest, an inhalation rate of 0.4 m^3 h^{-1}, or 111 cm^3 s^{-1} is assumed in this paper. Inhalation dose is given by the product of breathing rate, exposure duration, and airborne pathogen concentration.

Pujadas et al. (2020) reported the SARS-CoV-2 viral load measured in 1145 symptomatic patients. The overall mean $\log_{10}$ viral load was 5.6 copies per mL (SD 3.0), and median $\log_{10}$ viral load was 6.2 copies per mL. Riediker and Tsai (2020) surveyed data on the number of viral copies present in sputum and swab samples of individuals with COVID-19. Specifically, they used 1000 copies per mL to represent a low emitter, 10^6 copies per mL to represent a typical emitter, and 1.3×10^{11} copies per mL to represent a high emitter. A viral load of 1×10^9 copies per mL is assumed in this paper.

The infectious dose for SARS-CoV-2 is currently not known. A study by Watanabe et al. (2010) used animal studies and modeling of SARS spreading in an apartment complex in China to estimate the infectious dose for SARS-CoV-1 to be 280 viral particles to cause disease in 50% of the population. In this paper 50 viral particles are assumed to cause disease in 63% of the population. That is, according to the Wells-Riley equation (Riley et al., 1978), the infection risk (R, %) is given by

$$R = 100\left(1 - e^{-N/50}\right) \tag{21}$$

where N is the total number of viral particles deposited in the respiratory tract.

4. Single-region model with short stay time

4.1. Model overview

The simplest model to predict the possibility of aerosol virus transmission to an individual is a single-region model, shown in Fig. 1. In this simplified model there is a single air inlet (Junction J4) from the outside atmosphere and a single air outlet (J5) to the atmosphere, which represent all air flow into and out of the room, respectively. The individual of interest, for virus transmission, is represented by two regions and three junctions. The first junction (J1) represents a protective mask, if included, to filter and reduce the aerosol particles breathed in by the individual. The first region (Air Gap) represents the small gap between the mask, if worn, and the respiratory tract. The second junction (J2) represents the respiratory tract of the individual where virus particles can settle and attach to respiratory tissue leading to a potential infection. The second region represents the individual's lung with the final junction representing the individual's exhale. It is assumed in this model that all virus aerosols inhaled settle or attach in the respiratory tract (J2) and pose a risk of infection.

Table 3
Inhalation rates for different activity levels (Adams, 1993).

Activity	Inhalation rate, m^3 h^{-1}
Resting	0.49
Standing	0.54
Light exercise	1.38
Moderate exercise	2.35
Heavy exercise	3.30

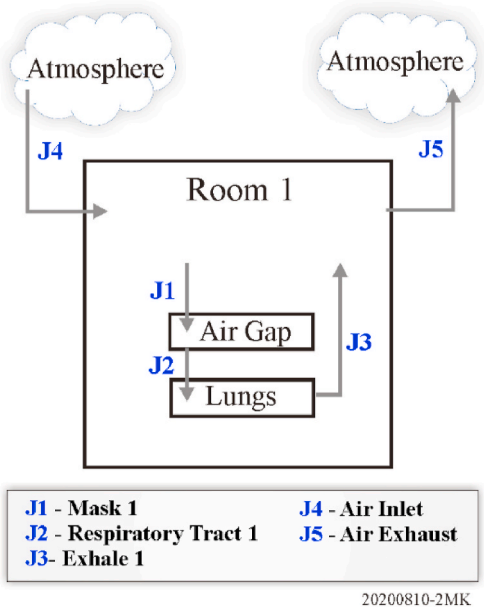

Fig. 1. Single-region model setup.

Since this model is focused on aerosol transmission within an enclosed space, the position of the source relative to the individual of interest is not a critical input; therefore, it has been neglected. The relative positioning of the source and individual of interest would be more critical for other means of virus transmission.

4.2. Results and discussion

In the single-region model, the virus emitter and the individual of interest occupy a 20-foot-square room with 12-foot ceiling, giving it a free volume of 4800 cubic feet or about 135.9 cubic meter. The emitter leaves after one half hour. The individual of interest stays in the room for another half hour. The room is ventilated at a rate of four air changes per hour (ACH), which is 320 cfm or 0.15 cubic meters per seconds. All the supplied air is from outside; no air is recirculated. The individual of interest wears a mask. The mask is assumed to provide 70% filtration efficiency. It is noted that mask efficiency is a range that depends on several factors (material, filter medium, the proper usage, etc.) which can impact the ultimate dose. In this analysis the dose is inversely proportional to the assumed filtration efficiency. Four cases are analyzed: 1. with no ventilation and no mask, 2. with ventilation but with no mask, 3. with no ventilation but with mask, and 4. with both ventilation and mask.

Fig. 2 shows the time history of aerosol mass distribution for case 4, with both ventilation and mask. Initially the mass of airborne aerosol increases linearly due to the constant aerosol production. The rate of increase slows down as the aerosol depletion increases due to gravitational settling, ventilation purge, and virus deactivation. The mass of aerosols deposited on the respiratory tract of the individual of interest continues to rise after the emitter leaves the room.

The rates at which the aerosols deposit on the mask and on the respiratory tract of the individual of interest are proportional to the mass of

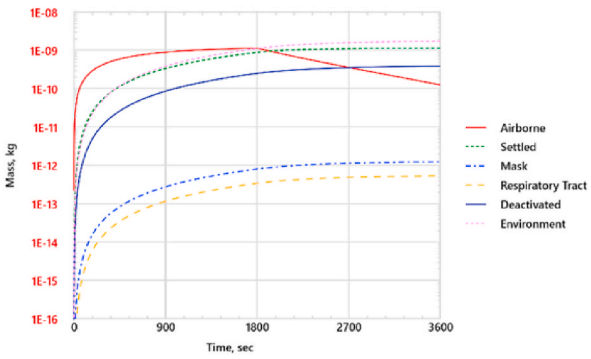

Fig. 2. Time history of aerosol mass distribution for case 4.

airborne aerosol. Clearly, a significant fraction of aerosols that could have ended up in the respiratory tract of the individual of interest is deposited on the mask, showing the effectiveness of wearing a mask in reducing the dose to the individual. At the end of 1 h, the individual of interest receives 5.78×10^{-13} kg of viral aerosols, or 5.78×10^{-10} mL. Since there are 10^9 virus particles in 1 mL, the individual receives 0.58 virus particles. The corresponding infection risk based on the Wells-Riley equation is 1.1%. The results for all four cases are summarized in Table 4.

The effectiveness of various measures taken to reduce the virus transmission is shown Fig. 3. As expected continuously purging the room atmosphere with outside air and wearing a mask are effective measures for reducing infection risk.

5. Multi-region model with long stay time

5.1. Model overview

Expanding upon the simplified model, the next logical step is to evaulate the possibility of virus aerosol tranmission in an interconnected multi-region scenario, shown in Fig. 4. In this model, two regions are interconnected; through a doorway (J1) and through a shared ventiliation system (J8 through J14).

The virus aerosol source is located within Room 1. Dose and infection risk for each of the three individuals of interest are considered. The individual in Room 1 (individual 1 of interest) and the individual in Room 2 (individual 2 of interest) are in the building with the emitter, the virus aerosol source, for the first 8 h. They leave the building after 8 h and the 2nd shift individual in Room 1 (Individual 3 of interest) enters Room 1 and stays for the next 8 h.

Realistic modeling of the ventiliation system is critical to modeling the aerosol transport between the two rooms. The system represents a majority of ventiliation systems which recondition, filter, and recycle the air rather than pulling fresh air directly from the atmosphere and exhausting air from within the region. This recirculation is done through junction 14 (J14) in Fig. 4. Half of the ventilated air (makeup air) is pulled in from the outside atmosphere (J8). An equivalent amount of air is exhausted from the regions through junction (J13). The remaining junctions in the ventilation system represent the air inflow (J9 and J10) from the inlet duct where fresh air is mixed with the recirculated air and air outlfow (J11 and J12) to the outlet ducts.

Three identical individuals are included in order to quantify the potential virus aerosol transmission in the system. The modeling for the individuals is identical to the simplified model with junctions J3, J6, and J16 representing the respiratory tracts, where virus can settle and attach leading to the potential for infection, of the three individuals of interest in Rooms 1 and 2.

Table 4
Summary of dose and infection risk results for single region model.

Case	Ventilation	Mask	HEPA	Dose 1, kg (Risk 1, %)
1	no	no	n/a	3.71×10^{-12} (7.1)
2	yes	no	n/a	1.58×10^{-12} (3.1)
3	no	yes	n/a	1.11×10^{-12} (2.2)
4	yes	yes	n/a	5.78×10^{-13} (1.1)

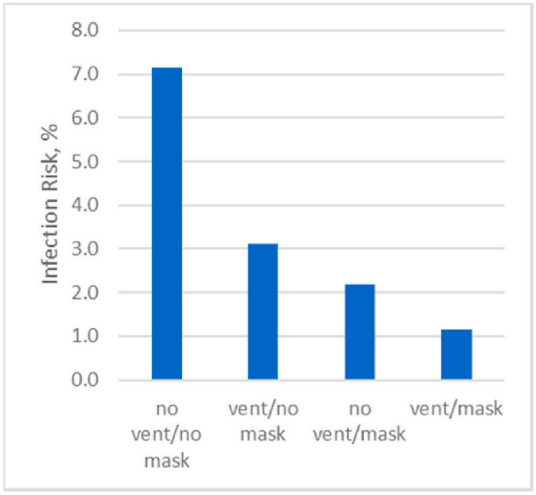

Fig. 3. Infection risks for single-region model.

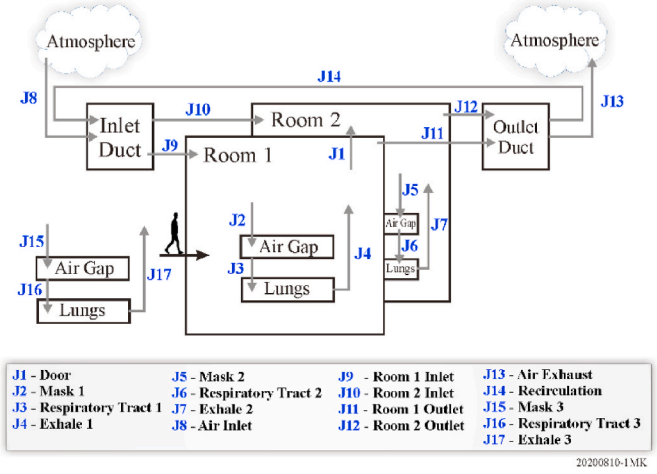

Fig. 4. Multi-region model setup.

5.2. Results and discussion

In the multi-region model, the virus emitter and the individual 1 of

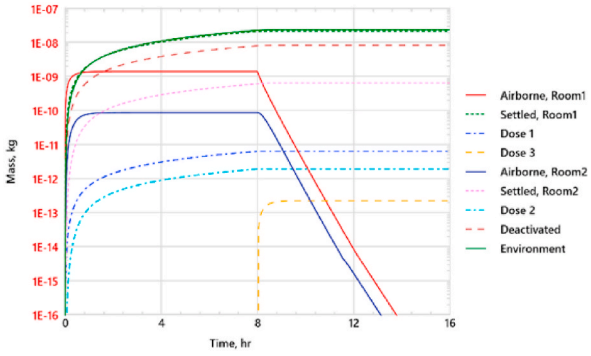

Fig. 5. Time history of aerosol mass distribution for case 6.

Table 5
Summary of dose and infection risk.

Case	Air Flow	Mask	HEPA	Dose 1, kg (Risk 1, %)	Dose 2, kg (Risk 2, %)	Dose 3, kg (Risk 3, %)
5	no	no	n/a	1.53×10^{-11} (26.4)	7.57×10^{-16} (<0.1)	1.83×10^{-12} (3.6)
6	yes	no	no	6.88×10^{-12} (12.9)	2.08×10^{-12} (4.1)	2.48×10^{-13} (0.5)
7	yes	no	yes	4.97×10^{-12} (9.5)	1.71×10^{-17} (<0.1)	1.11×10^{-13} (0.2)
8	yes	yes	yes	1.78×10^{-12} (3.5)	1.20×10^{-17} (<0.1)	3.32×10^{-14} (0.1)

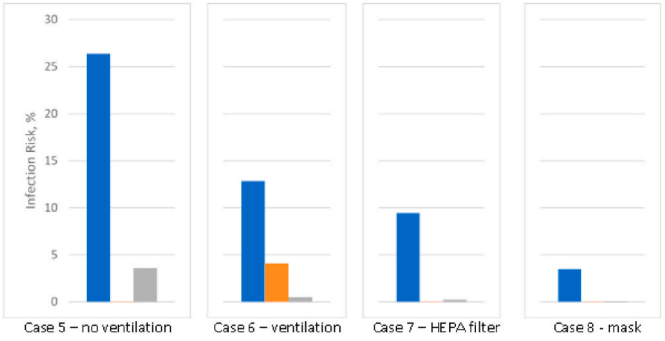

Fig. 6. Infection Risks for Multi-Region Model (blue: individual in Room 1, orange: individual in Room 2, grey: 2nd shift individual in Room 1). (For interpretation of the references to colour in this figure legend, the reader is referred to the Web version of this article.)

interest are in Room 1 (679.6 cubic meter). The individual 2 of interest is in Room 2 (135.9 cubic meter). After 8 h, the virus emitter, individua1 1 of interest, and individual 2 of interest leave the building and the 2nd shift individual (individual 3 of interest) enters Room 1 and stays for the next 8 h as shown in Fig. 4.

Both rooms share a ventilation system. The rooms are ventilated at a rate of four air changes per hour (ACH), with half of the air recirculated. Four cases are analyzed: 5. with no ventilation and no mask, 6. with ventilation and no mask, 7. with a HEPA filter on the recirculated air and no mask, and 8. with both a HEPA filter and mask.

Fig. 5 shows the distribution of aerosol mass for case 6, with ventilation and no mask. The aerosol removal rates by gravitational settling and by ventilation are nearly identical. The aerosol removal by virus deactivation is significant, albeit smaller than the gravitational settling or by ventilation. Although the aerosol source is in Room 1, the aerosols are transported to Room 2 by the recirculated air through shared ventilation ducts and the individual 2 of interest in Room 2 receives appreciable dose.

After the virus aerosol emitter leaves the building, the aerosol concentrations decay exponentially. Individual 3 of interest, who enters Room 1 after the emitter leaves the building, is exposed to the room atmosphere loaded with virus aerosols and receives a small but non-negligible dose. At the end of 16 h, the three individuals of interest have received 6.88×10^{-12} kg, 2.08×10^{-12} kg, and 2.48×10^{-13} kg of viral aerosols, with corresponding infection risk of 12.9%, 4.1%, and 0.5%, respectively. The results for all four cases are summarized in Table 5. The effectiveness of various measures taken to reduce the virus transmission is shown in Fig. 6. As expected, ventilation, with HEPA filters for recirculated air, and wearing masks reduce the infection risk. Without HEPA filters, the recirculated air can spread virus aerosols to other rooms sharing the same ventilation system.

6. Conclusions and future research

A mechanistic model is developed to quantify airborne transmission and infection of SARS-CoV-2 using the facility modeling code FATE. The model is applied to single-region and multi-region settings. Some key information about the pathogen such as the infectious dose of SARS-CoV-2 is not known. Some input such as the viral load varies greatly between individual emitters. Hence, the infection risks reported in this paper are valid for specific inputs assumed and should not be taken literally. On the other hand, the model can be used to quantify the effectiveness of various measures taken to reduce the airborne transmission of the virus as the model can be easily modified to represent different confinement settings and ventilation networks.

As expected, the FATE model shows that for a single room continuously purging the room atmosphere with outside air and wearing masks are effective measures for reducing infection risk. For a multi-room facility, ventilation, with HEPA filters for recirculated air, together with wearing masks reduces the infection risk. Without HEPA filters, the recirculated air can spread virus aerosols to other rooms sharing the same ventilation system. The FATE model is easily modified to accommodate alternate system design or performance characteristics to quantify the benefit of system modifications in reducing infection risk. Hence, the virus loading always responds in expected ways to the model input parameters air changes per hour (ACH) and virus half life, which appear as linear droplet removal rate terms in the governing equations. The utility of the model is that the expected trends, that is the effects of these parameters on virus loading and infection risk, can now be quantified.

The analysis presented here provides a narrowly focused scope on the potential risk infection from a quasi-steady state virus aerosol generation through breathing. Several mitigation strategies were also presented to reduce the infection risk within the facility. Future research on this topic will continue to expand the knowledge basis on virus aerosol transmission within a facility and provide additional guidance on mitigation strategies. As more data becomes available on the SARS-CoV-2 virus (aerosol size distributions, interaction within the respiratory tract, virus half-life, etc.) the analysis inputs will be based on distributions improving the independency of the analysis from the specific inputs currently assumed. The scope of the analysis can be expanded to include sporadic aerosol generation through mechanisms of coughing and sneezing. Future research on the local flow field and inertia of virus droplets flowing around the head will improve the physical prediction of the infection risk due to an individual inhaling virus loaded air within the facility.

Credit author statement

Matthew Kennedy: Conceptualization, Methodology, Project Administration, Funding Acquisition, Writing – Original & Review;

Sung Jin Lee: Conceptualization, Methodology, Formal Analysis, Software, Writing – Original & Review; **Michael Epstein:** Methodology, Validation, Investigation, Writing – Original & Review.

Declaration of competing interest

The authors declare that they have no known competing financial interests or personal relationships that could have appeared to influence the work reported in this paper.

Acknowledgements

The authors would like to extend a deep thank you to the management (Zach Hachmeister, Ken Kurko, Ashok Dastidar, Marty Plys, Jim Burelbach, and Jacky Shoulders) at Fauske and Associates LLC for supporting this effort and the countless discussions which provided guidance while developing this content.

References

Adams, W.C., 1993. Measurement of breathing rate and volume in routinely performed daily activities. In: Final Report, Contract No. A033-205, Human Performance Laboratory, Physical Education Department, University of California, Davis, Prepared for the California Air Resources Board, April.

Asadi, S., Wexler, A.S., Cappa, C.D., Barreda, S., Bouvier, N.M., Ristenpart, W.D., 2019. Aerosol emission and superemission during human speech increase with voice loudness. Sci. Rep. 9, 2348.

Buonanno, G., Stabile, L., Morawska, L., 2020. Estimation of airborne viral emission: quanta emission rate of SARS-CoV-2 for infection risk assessment. Environ. Int. 141.

Cheesewright, R., 1968. Turbulent natural convection from a vertical plane surface. J. Heat Tran. 90, 1–8.

Epstein, M., Ellison, P.G., Henry, R.E., 1986. Correlation of aerosol sedimentation. J. Colloid Interface Sci. 113, 342–355.

Epstein, M., Ellison, P.G., 1988. Correlations of the rate of removal of coagulating and depositing aerosols for application to nuclear reactor safety problems. Nucl. Eng. Des. 107, 327–344.

Epstein, M., 2002. Calculation of Spherical Particle Terminal Velocity unpublished FAI Memo, July 3.

Morawska, L., Johnson, G.R., Ristovski, Z.D., Hargreaves, M., Mengersen, K., Corbett, S., Chao, C.Y.H., Li, Y., Katoshevski, D., 2009. Size distribution and sites of origin of droplets expelled from the human respiratory tract during expiratory activities. J. Aerosol Sci. 40, 256–269, 2009.

Pujadas, E., Chaudhry, F., McBride, R., Richter, F., Zhao, S., Wajnberg, A., Nadkarni, G., Glicksberg, B.S., Houldsworth, J., Cordon-Cardo, C., 2020. SARS-CoV-2 viral load predicts COVID-19 mortality. correspondence LANCET Respiratory Med. August 6.

Riediker, M., Tsai, D.H., 2020. Estimation of viral aerosol emissions from simulated individuals with asymptomatic to moderate coronavirus disease 2019. JAMA Network Open. July 1.

Riley, E.C., Murphy, G., Riley, R.L., 1978. Airborne spread of measles in a suburban elementary school. Am. J. Epidemiol. 421–432.

van Doremalen, N., Bushmaker, T., Morris, D.H., Holbrook, M.G., Gamble, A., Williamson, B.N., Tamin, A., Harcourt, J.L., Thornburg, N.J., Gerber, S.I., Lloyd-Smith, J.O., de Wit, E., Munster, V.J., 2020. Aerosol and surface stability of SARS-CoV-2 as compared with SARS-CoV-1," correspondence. N. Engl. J. Med. 382, 1564–1567. April 16.

Watanabe, T., Bartrand, T.A., Weir, M.H., Omura, T., Haas, C.N., 2010. Development of a dose-response model for SARS coronavirus. Risk Anal. 30 (7), 1129–1138.

World Health Organization, 2020. Transmission of SARS-CoV-2: implications for infection prevention precautions. Scientific Brief. July 9.